
UPPER ATMOSPHERE RESPONSE TO EXTRATROPICAL CYCLONES

V.I. Zakharov 

*Lomonosov Moscow State University,
Moscow, Russia, Zvi_555@list.ru
Schmidt Institute of Physics of the Earth RAS,
Moscow, Russia
Obukhov Institute of Atmospheric Physics RAS,
Moscow, Russia*

M.S. Solovieva

*Schmidt Institute of Physics of the Earth RAS,
Moscow, Russia, roznoi@ifz.ru*

S.L. Shalimov

*Schmidt Institute of Physics of the Earth RAS,
Moscow, Russia, pmsk7@mail.ru
Space Research Institute RAS,
Moscow, Russia*

M.G. Akperov

*Obukhov Institute of Atmospheric Physics RAS,
Moscow, Russia, aseid@ifaran.ru*

G.M. Korkina

*Kamchatka Branch, Unified Geophysical Service of the
Russian Academy of Sciences Federal Research Center,
Petropavlovsk-Kamchatsky, Russia, gkor@emsd.ru*

N.R. Bulatova

*Kamchatka Branch, Unified Geophysical Service of the
Russian Academy of Sciences Federal Research Center,
Petropavlovsk-Kamchatsky, Russia, geofizik@emsd.ru*

Abstract. We have examined the response of the lower and upper ionosphere to the passage of extratropical cyclones in 2014–2023, using measurements made at regional ultra-long-wave radio stations and satellites of the Swarm mission in the Far Eastern region of Russia. For twelve cyclones, we have found that disturbances in the lower ionosphere, observed in VLF signal amplitude and phase variations, as well as their associated electron density variations in the upper ionosphere during the active stage of the cyclones, correspond to the passage of atmospheric internal gravity waves and

their dissipation, as evidenced by several examples. We have studied the mechanisms of the influence of internal atmospheric waves on the ionosphere, which make it possible to interpret the VLF signal phase variations observed in the lower ionosphere and the electron density variations in the upper ionosphere.

Keywords: ultra-long-wave radio sounding, atmospheric internal gravity waves, extratropical cyclones, ionosphere.

INTRODUCTION

Studying the interaction between Earth's outer layers (atmosphere, ionosphere, magnetosphere), which is manifested when there are high-energy sources in one of these geospheres, as well as mechanisms of such relationships, is one of the important tasks of contemporary geophysics.

According to [Forbes et al., 2000], the influence of atmospheric (meteorological) factors under quiet geomagnetic conditions can be as great as 35 % of the background level for disturbances in the upper atmosphere (specifically, the electron density N_e at the maximum of the ionospheric F2 layer located at 250–300 km). Atmospheric internal gravity waves (IGWs) are considered to be the crucial link connecting meteorological factors with the ionosphere [Danilov et al., 1987]. In particular, calculated azimuths and horizontal velocities of some traveling ionospheric disturbances (TIDs) of meteorological origin (which are commonly associated with propagating IGWs) have shown that probable zones of generation of recorded TIDs are located in the troposphere and coincide, for example, with depressions in cyclone formation areas [Bertin et al., 1975]. Atmospheric waves generated by meteorological events, when propagating upward, pass through both the lower and

upper ionosphere. Accordingly, disturbances during cyclones should be observed in both the lower and upper ionospheres.

Indeed, when studying tropical cyclones (typhoons), a possible response is found not only in the lower ionosphere from rocket experiment results [Vanina-Dart et al., 2008] and VLF radio sounding [Roznoi et al., 2014; Pal et al., 2020; Das et al., 2021; Shalimov, Solovieva, 2022], but also in the upper ionosphere from results of analysis of GPS signals [Polyakova, Perevalova, 2011; Zakharov, Kunitsyn, 2012; Yasyukevich et al., 2013; Vanina-Dart, Sharkov, 2016; Chou et al., 2017a, b], satellite measurements [Zakharov et al., 2019; Shalimov et al., 2023a, b], and oblique ionospheric sounding data [Chernigovskaya et al., 2010]. At the same time, the response of the upper atmosphere to extratropical cyclones, unlike tropical ones (see, e.g., the review [Chernogor, 2023]), have not been studied systematically because of the difficulty in isolating the atmospheric feature per se. It is necessary to continue research on the response of the atmosphere to the passage of a cyclone of any type, using capabilities of various monitoring tools, which can facilitate determining the mechanisms of cyclone effects on the ionosphere, which have received attention only recently.

Extratropical cyclones are recorded at middle and high latitudes [Khromov, Petrosyants, 2006; Lutgens et al., 2018; Shved, 2020]. One of the main, but not the only, mechanisms of their origin is the baroclinic instability of the atmosphere — dynamic wave instability of atmospheric current with a latitudinal temperature gradient and hence with a vertical wind velocity gradient in the Coriolis force field. The energy source of growing disturbances in such a current is the available potential instability energy. Regardless of the formation mechanisms, cyclones always manifest themselves as closed isobars on the atmospheric pressure map, and their formation and evolution are accompanied by changes in wind and related tropospheric disturbances, including wave ones.

To calculate cyclone characteristics at extratropical latitudes ($>20^\circ$ N) of the Northern Hemisphere, we have used 6-hr mean sea level pressure from ERA-5 reanalysis data and a method of identifying cyclone characteristics [Bardin, Polonsky, 2005; Akperov et al., 2007]. Cyclones are defined as low pressure areas bounded by closed isobars. The cyclone characteristics such as the number of cyclones, their lifetime, depth (intensity), determined by the difference between minimum pressure in a cyclone and the value on the last closed isobar, the area occupied by the cyclone, and the size of the cyclone, i.e. its mean radius, are calculated. The square of cyclone intensity is characterized by the kinetic energy of the cyclone [Golitsyn et al., 2007; Simmonds, Keay, 2009]. Comparison of the statistics of cyclone characteristics obtained by this method [Akperov et al., 2007, Golitsyn et al., 2007] and other identification methods [Neu et al., 2013; Ulbrich et al., 2013] shows their close agreement. The number of extratropical cyclones, comparable and superior to tropical ones, is by an order of magnitude larger than that of tropical events per year.

When extratropical cyclones move above water surface, we can expect wave responses in the ionosphere, similar to those observed from tropical cyclones moving generally above water. That is why we have chosen the region of the Pacific Ocean and the Far East for our research, where cyclones are most frequent and there is a significant fraction of sea or ocean surface, as well as several VLF radio paths.

Figure 1 illustrates distribution of large extratropical cyclones for 2020–2023, characterized by a pressure drop of more than 10 hPa, a duration of more than three days, and a maximum diameter of more than 300 km, which corresponds to the size of tropical cyclones.

The size of extratropical cyclones at sea level is seen to be, on average, ~ 1500 km, which exceeds that for tropical cyclones. Below, we present meteorological data on individual extratropical cyclones.

In this paper, we have for the first time employed measurements made by a regional network of VLF radio sounding stations (recording disturbances in the lower ionosphere) and data from the Swarm satellite mission (recording disturbances in the upper ionosphere) in order to study the ionospheric response to extratropical cyclones. This approach makes it possible to use the

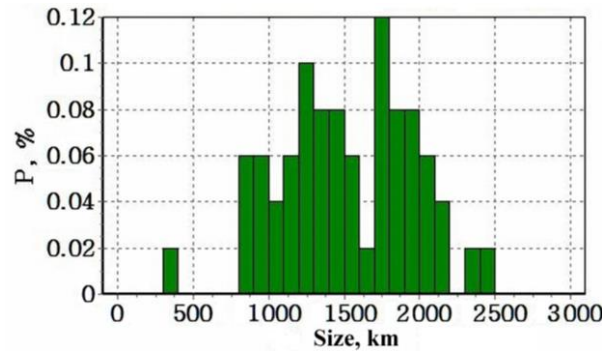


Figure 1. Distribution of large extratropical cyclones with a pressure drop >10 hPa, a duration of more than three days, and a maximum diameter >300 km for the Far East region in 2020–2023

unique capabilities of various observation methods and monitor the development of an atmospheric disturbance caused by an extratropical cyclone at different ionospheric heights as the disturbance spreads. This approach also allows us to specify the mechanisms of cyclones' impact on the ionosphere.

EXPERIMENTAL RESEARCH METHODS

The response of the lower ionosphere to atmospheric processes is studied by the method of remote VLF radio sounding at frequencies 3–30 kHz the signals at which can propagate thousands of kilometers from a transmitter to a receiver with weak damping of ~ 2 dB per 1000 km in the natural Earth–ionosphere waveguide. Reflection from the upper wall of the waveguide (the ionosphere) occurs at altitudes of ~ 65 km during the day and ~ 85 km at night. Signal amplitude and phase are sensitive indicators of the state of the ionosphere. Wave disturbances, generated in the atmosphere by a fairly strong cyclone, when propagating into the upper ionosphere should pass through the lower ionosphere, which is indicated by corresponding VLF-signal amplitude and phase disturbances.

We have used data from the Unique Research Facility "Seismic and Ultrasonic Monitoring Complex of the Arctic Cryolithozone and Continuous Seismic Monitoring Complex of the Russian Federation, Neighboring Territories, and the World" [Dyagilev, Sdelnikova, 2022; <https://ckp-rf.ru/usu/507436/>; <http://www.gsras.ru/unu>]. Receiving stations of VLF radio sounding of the regional network in the Russian Far East are located in Petropavlovsk-Kamchatsky, Yuzhno-Sakhalinsk, and Yuzhno-Kurilsk. The stations are equipped with UltraMSK receivers [<http://ultramsk.com>], which can simultaneously measure the amplitude and phase of MSK (Minimum Shift Keying) modulated signals in the frequency band 10–50 kHz from several transmitters. The MSK signals have fixed frequencies in the range 50–100 Hz relative to the fundamental frequency. The receiver can receive signals with a sampling step from 50 ms to 60 s. The analysis is based on data averaged over a time interval of 20 s.

We have analyzed VLF-signal variations for 48 extratropical cyclones from 2014 to 2023, which crossed the sensitivity zones of paths (five Fresnel zones) in the absence of magnetic and seismic activity (i.e. for events with $M > 5.5$). The effects have been detected for 12 events. The paths were signals from NWC (19.8 kHz) transmitter on the west coast of Australia and JJY (40 kHz) and JJI (22.2 kHz) transmitters in Japan, received at stations in Petropavlovsk-Kamchatsky (PTK), Yuzhno-Sakhalinsk (YSH), and Yuzhno-Kurilsk (YUK). Data on the cyclones was obtained using the IAPh RAS (Institute of Atmospheric Physics of the Russian Academy of Sciences) method described in the previous section.

We analyzed the night time interval since the day-side ionosphere is very stable and sensitive only to severe impacts such as solar flares and magnetic storms [Kleimenova et al., 2004]. VLF signals have diurnal and seasonal variations; therefore, in the analysis we compared observed and monthly average signals.

To study disturbances in the upper ionosphere, which are synchronous with those observed in the lower ionosphere by microwave radio sounding, we have used data from three Swarm satellites (A, B, and C) located in two circumpolar orbits: the orbits of Swarm A and C have an inclination of 87.4° at almost the same altitude (430–460 km for 2019) and move in similar orbits with an orbital difference 2–10 s. The third satellite has different motion parameters (for example, the orbit in the altitude range 500–540 km), is not synchronized with the first satellites, and is a reference satellite [Olsen et al., 2013]. We employ data on space-time electron density distribution from satellite Langmuir probes with a sampling rate of 2 Hz and a relative error in the maximum electron density no more than 1 % when the satellites flew over typhoon zones. The data is available at [<http://directory.eoportal.org/web/eoportal/satellite-missions/s/Swarm>].

Since the size of the cyclone area in the atmosphere is on average 1500 km, taking into account the Swarm satellite velocity we have selected the time filter parameters in the range from 15 s to 5 min.

The search for flyby data reduces to determining the intersection of projections of satellite tracks with the region where ionospheric effects of cyclones can be observed. This work has been carried out using dedicated software developed at the Faculty of Physics of Moscow State University. All the figures presented in this section have been obtained with a semi-automatic processing complex, using a method for studying tropical cyclones. The response recording features are similar to those of the problem for tropical cyclones.

Note that we search for ionospheric responses at night when the effect of the ionosphere on propagation of VLF signals is the most significant. Yet, at this time the electron density, which is utilized as an indicator of disturbances in the ionosphere, decreases. Finally, when an extratropical cyclone as a source of IGW generation approaches land, the pattern of recorded disturbances can change due to wave interference. All this causes additional difficulties, along with the lack of flybys during the period of interest in the immediate vicinity of the

cyclone or typhoon region and the difficulties in identifying the response against the background of natural ionospheric disturbances.

MEASUREMENT RESULTS

Thus, it is difficult to observe synchronous disturbances in the lower and upper ionosphere during cyclones due to the fact that the nightside ionosphere is considered in measurements made by VLF radio sounding, and the almost synchronous flybys of Swarm satellites may be shifted in time by ~ 5 –7 hrs. Nevertheless, in this paper disturbances of the lower and upper ionosphere are examined for one case of almost synchronous measurements and several cases with the given time delay.

Let us analyze the manifestation of the atmosphere-ionosphere coupling during the cyclone that occurred on June 20 – July 3, 2016. Figure 2 illustrates a pressure change (its drop by 18 hPa) against the background of moderate geomagnetic disturbance: $Dst < 25$ nT, $K_p < 3$, except for the 6-hour interval on the night of June 23.

For the event numbered 2008611 (18) from the IAPh RAS catalog, we have analyzed two paths: JJY–PTK and NWC–YSH, with high-quality data for June 20 – July 03, 2016. The map is presented in Figure 3. Signal amplitude and phase disturbances along the NWC–YSH path were recorded on June 24.

Figure 4 shows the signal amplitude and phase for the NWC–YSH path on June 24, 2016, compared with the monthly average level. Two features of signal phase variations can be observed: a rather long (several hours) negative phase shift, which is replaced by a positive anomaly, and shorter-period wave variations superimposed on them. There is a negative amplitude anomaly. The phase shift is 40° – 50° . The wavelet analysis indicates that short-period amplitude and phase variations have the main period of ~ 30 min.

For the JJY–PTK path (see Figure 5), the effect was observed on June 27, 2016. When comparing phases, June 20 is used as a quiet day. There is also a wave-like phase variation. The deviation from the signal level on the quiet day is as large as 40° . Wavelet analysis of a signal from the JJY transmitter in Kamchatka on July 27 also shows the presence of 30-min variations.

The track of Swarm B when it flies over cyclone 2008611(18), as well as the relative range of the cyclone and electron density variations for June 24, 2016 between 20:50 and 21:02 UT are shown in Figure 6. Variations in the relative electron density are as great as 10 %.

Tracks of the Swarm satellites along with electron density variations for the same cyclone, but for June 27, 2016 between 16:09 and 16:22 UTC are exhibited in Figure 7. While Swarm A and C are synchronized in space and time, i.e. they enter neighboring regions that are less than 1.5 apart in longitude and differ in time by 2–10 s, the responses are not synchronous. The correlation between signals from these satellites is, generally, at least 0.85, but in this case the correlation is low, which may indicate the formation of various regions in the ionosphere along the satellite tracks due to quasi-wave plasma motions, wave interference, or local plasma turbulence.

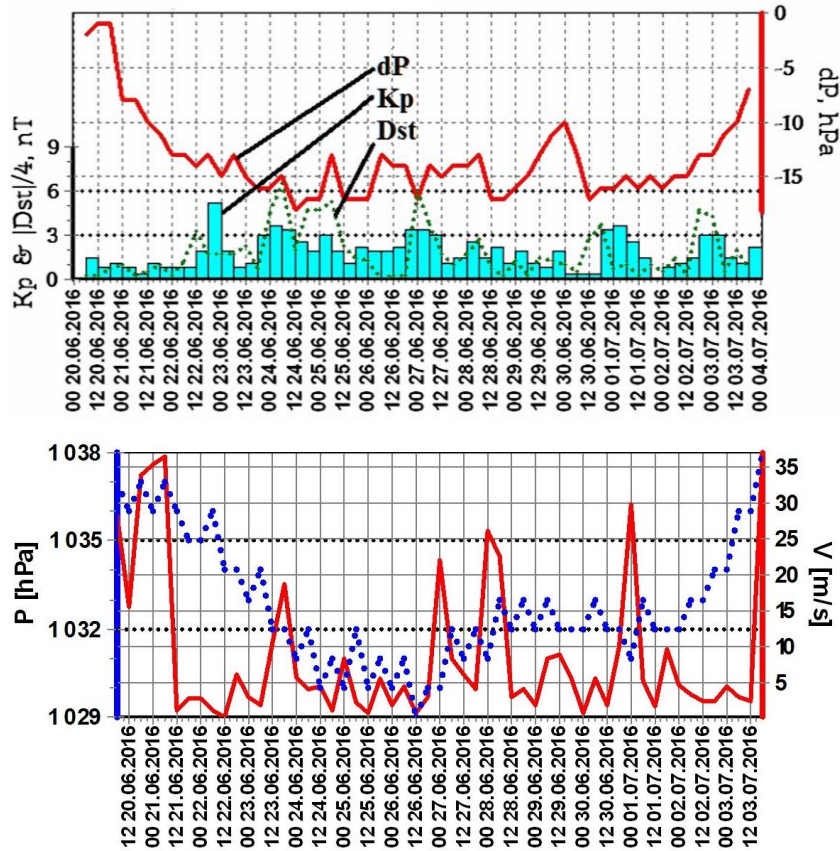


Figure 2. Time evolution of the cyclone on June 20 – July 3, 2016 (event 2008611(18) with a pressure drop dP of 18 hPa according to the IAPh RAS catalog) and behavior of the geomagnetic indices K_p and $|Dst|$ (a), as well as pressure and wind speed variations during the event of interest (b)

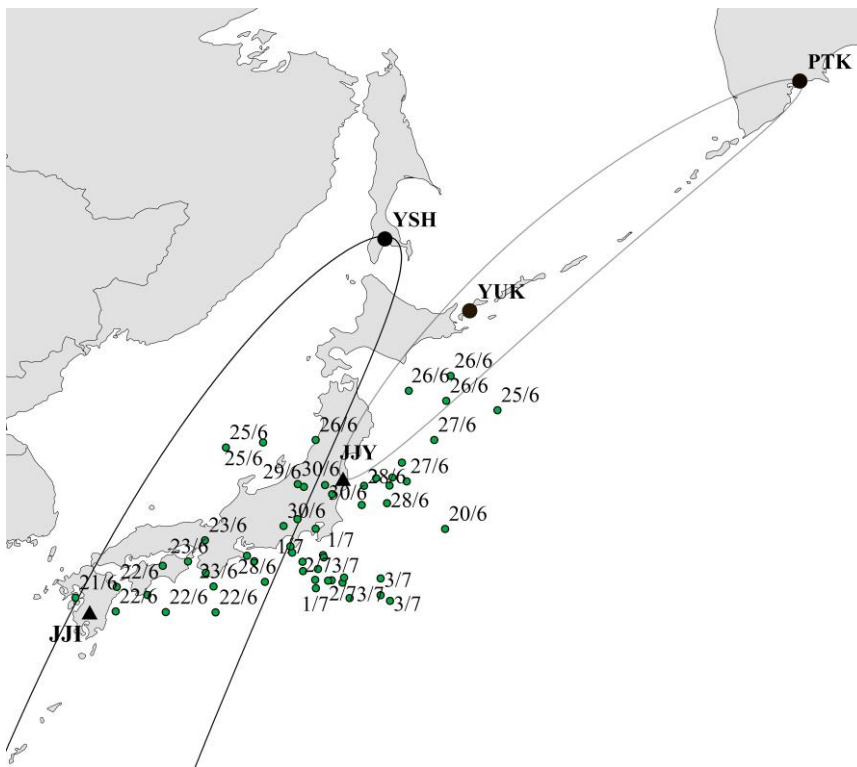


Figure 3. Movement of cyclone 2008611(18) (dots) and position of PTK (Petropavlovsk-Kamchatsky), YSH (Yuzhno-Sakhalinsk), YUK (Yuzhno-Kurilsk) receivers and JJI (22.2 kHz) and JJY (40 kHz) transmitters: the ellipse indicates projection of five Fresnel zones onto Earth's surface (the sensitivity zone of the NWC–YSH path is partially shown); numbers are dates in the day/month format

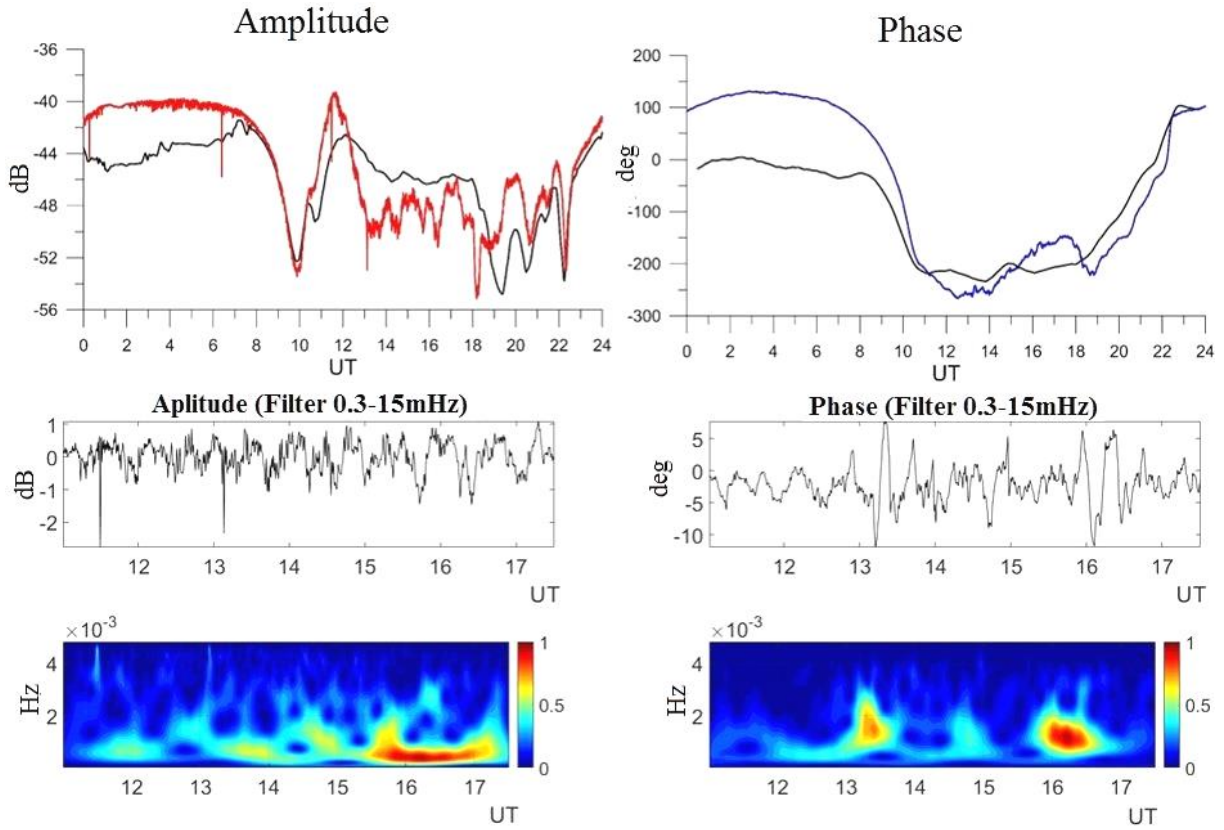


Figure 4. Amplitude and phase of a signal from the NWC transmitter at the station in Yuzhno-Sakhalinsk on June 24, 2016: in top panels are signal amplitude and phase variations; black lines indicate monthly averages; in middle panels are the filtered-signal amplitude and phase at night; in bottom panels are wavelet spectra of the filtered signal

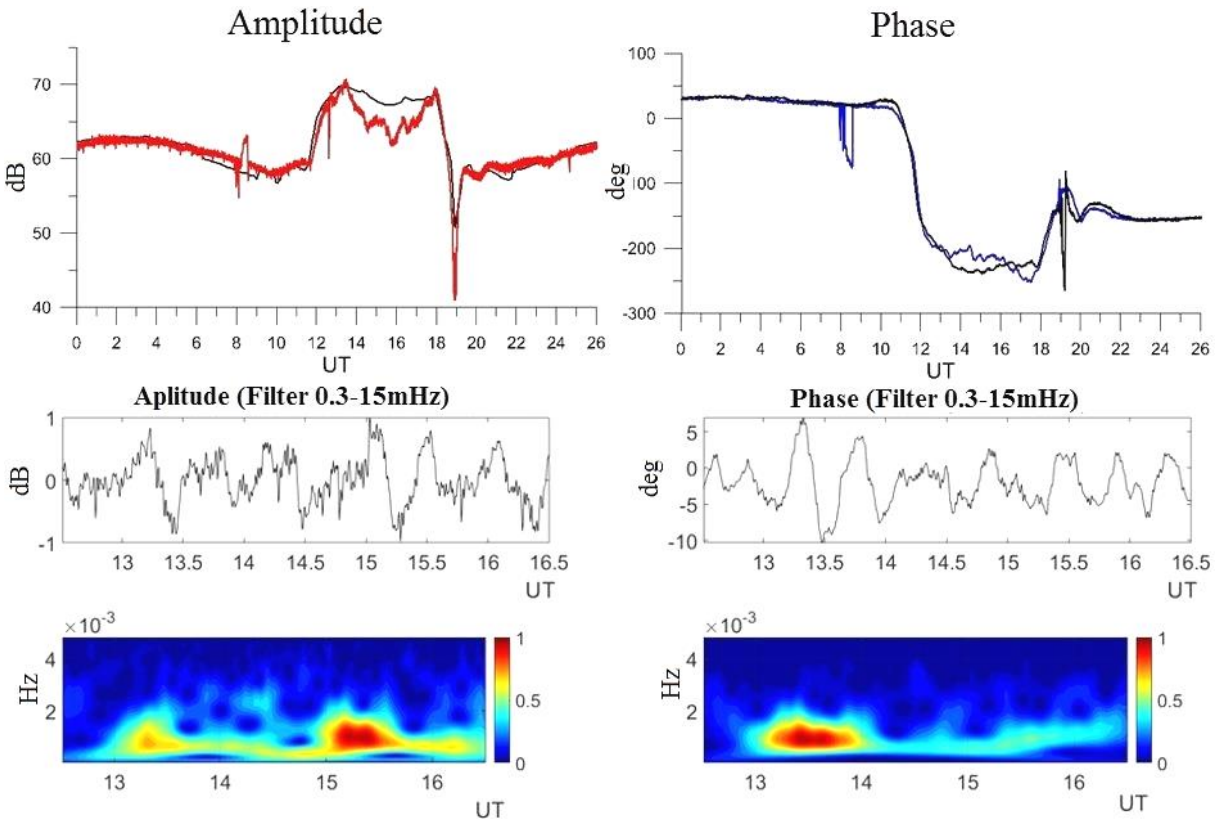


Figure 5. Amplitude and phase of a signal from the JJY transmitter at the station in Petropavlovsk-Kamchatsky on June 27, 2016. Notations are similar to those in Figure 4

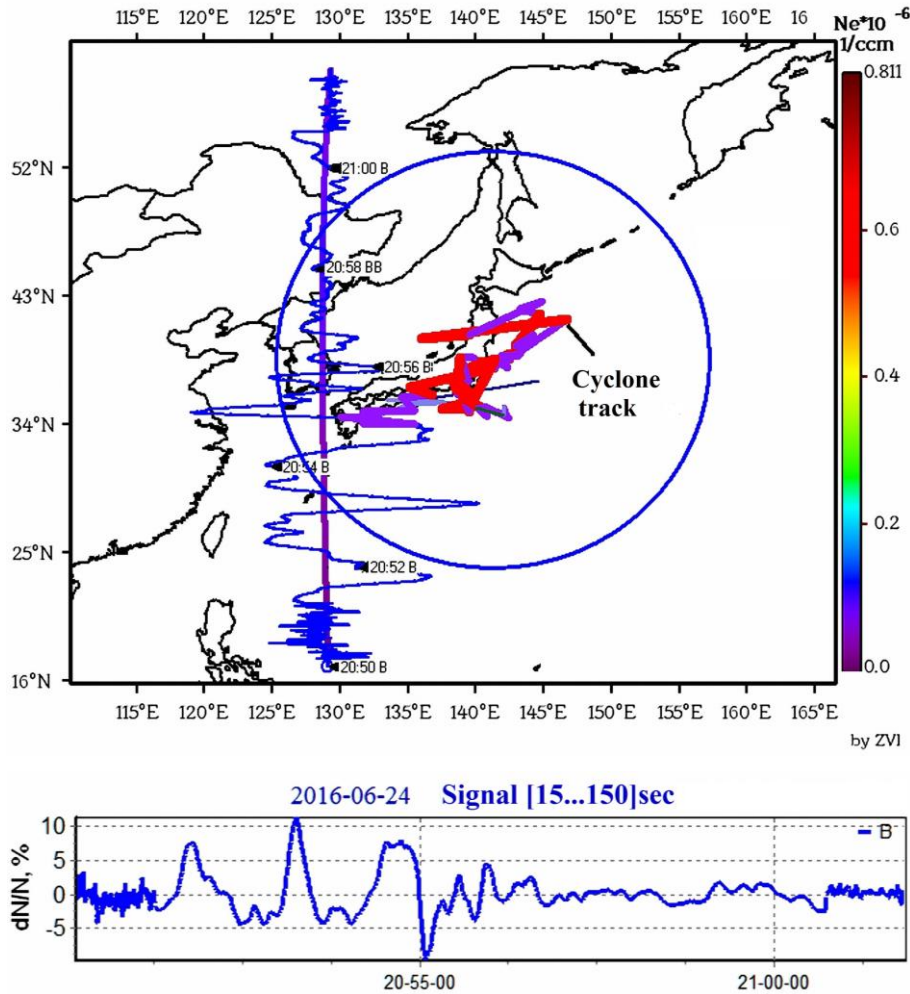


Figure 6. Panel *a* illustrates spatiotemporal electron density disturbances along the track of Swarm B over cyclone 2008611(18) on June 24, 2016 at 20:50–21:02 UTC. Also shown is the relative range of the cyclone and its track over the entire period of its existence. The projection of the satellite track onto Earth's surface is marked with a ray around which there are relative electron density variations. Panel *b* shows relative electron density variations for a time interval to 3 min at 530 km (height of Swarm-B orbits)

For another event, cyclone 914245(16) from the IAPh RAS catalog with a pressure drop of 16 hPa, we analyzed only the JJY signal for July 01— July 06, 2020 since the rest of the data was of poor quality. The effects were found for July 06, 2020. Figure 8 shows the cyclone's location in time and analyzed VLF paths.

Recordings of the VLF signal amplitude and phase for the JJY-PTK path and the corresponding wavelet maps for the signal filtered in the frequency band 0.3–15 MHz are presented in Figure 9. Two features of signal phase variations can be observed: a rather long (several hours) positive phase shift, which is replaced by a negative anomaly (i.e. the variation is inverse to that shown in Figures 4 and 5), and shorter-period wave variations superimposed on them.

Let us now analyze Swarm satellite measurements in the upper ionosphere. Figure 10 presents the result of measurement of electron density variations by Swarm A and C on July 06, 2020 at 15:43–15:52 UTC over the cyclone area, approximately at the same time when the VLF-signal variations exhibited in Figure 9 were recorded. The map shows the entire track of the cyclone throughout the period of its action. The ellipse in the

map projection marks the area of the storm during the given time period. Rays indicate projections of satellite tracks onto Earth's surface.

The electron density responses detected in the range 15...180 along the tracks are shown in Figure 10, *b*. Pay attention to the detected quasi-wave structures of a sufficiently high (to 30 %) relative amplitude dN/N . Taking into account the satellite velocity (~ 7.5 km/s), the length of the structures is 400–600 km, which is of the same order of magnitude as the horizontal wavelength of the structures.

DISCUSSION AND CONCLUSIONS

As already noted, there are two features of VLF-signal phase variations: long-period (several hours) negative and positive anomalies on which shorter-period wave variations are superimposed.

The experimental data presented does clearly demonstrate wave disturbances of VLF-signal amplitude and phase during the active stage of cyclones, i.e. the presence of wave disturbances in the lower ionosphere.

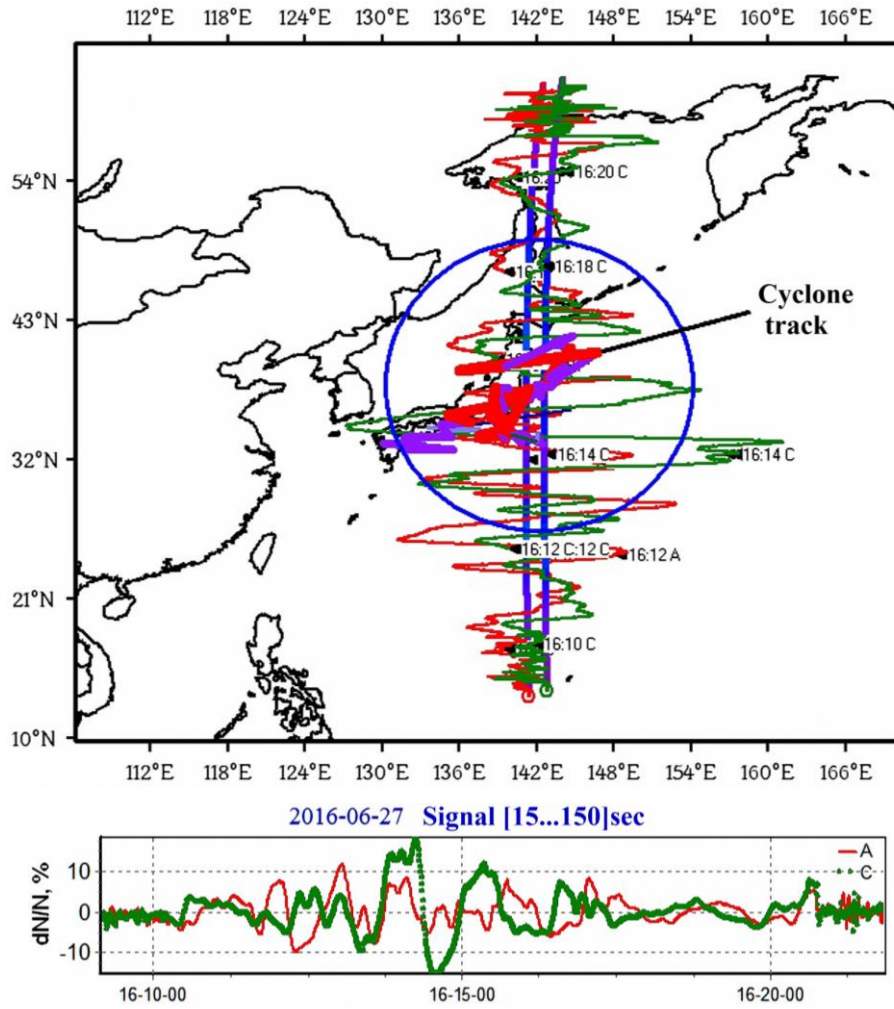


Figure 7. Panel a illustrates spatiotemporal electron density disturbances along the tracks of Swarm A and C over cyclone 2008611(18) on June 27, 2016 at 16:09–16:22 UTC. The notations are similar to those in Figure 6. In panel b are variations in the relative electron density for a time interval to 3 min at 460 km (height of Swarm-A and -C orbits)

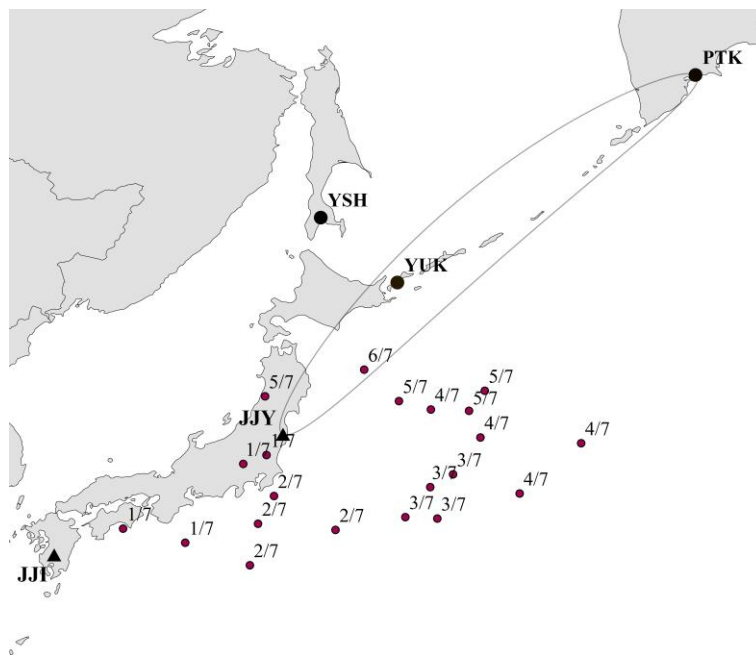


Figure 8. The same as in Figure 3 for cyclone 914245(16)

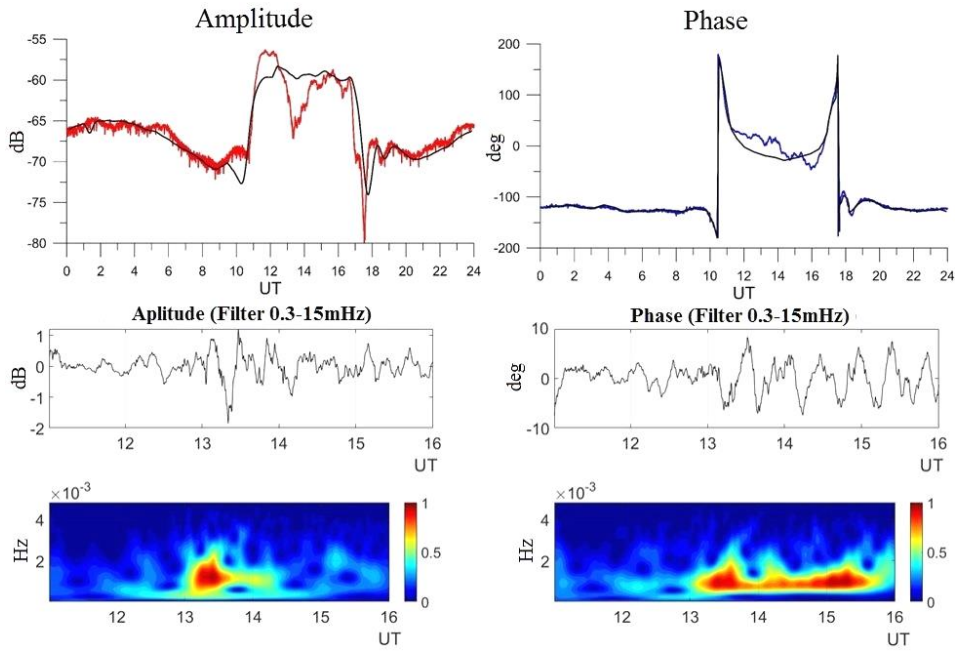


Figure 9. In top panels are the JJY signal amplitude and phase variations recorded at the station in Petropavlovsk—Kamchatsky on July 6, 2020: black lines are monthly averages. Middle panels represent the amplitude and phase of the filtered signal at night. Bottom panels exhibit wavelet spectra of the filtered signal

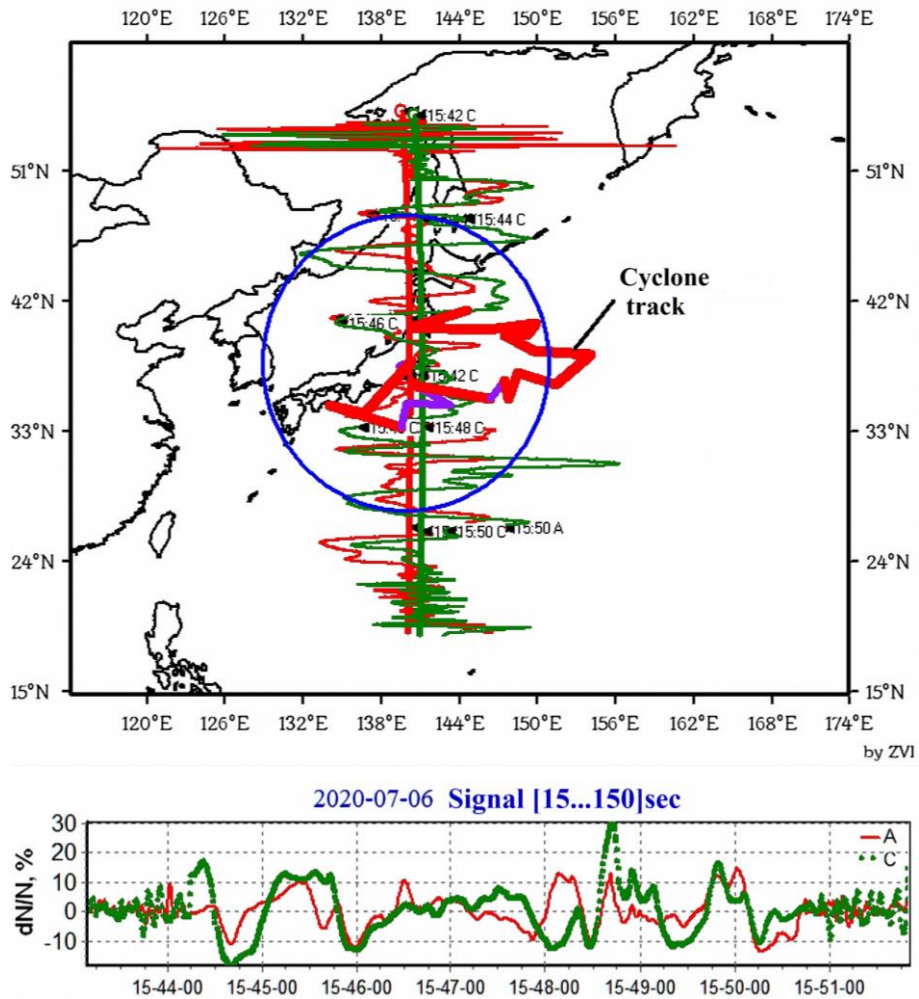


Figure 10. In panel a are spatiotemporal electron density disturbances along the tracks of Swarm A and C over cyclone 914245(16) on July 06, 2020 at 15:43–15:52 UTC. The notations are similar to those in Figure 6. In panel b are variations in the relative electron density at 460 km (height of Swarm-A and -C orbits)

Wavelet analysis shows the presence of wave activity within the range of 8–55 min periods (see Figures 4, 5, 9). This range corresponds to atmospheric internal gravity waves (IGWs).

If we turn to Swarm observations (see Figure 10), which are almost synchronous with recording of disturbances through VLF radio sounding, we can see that the satellite records ionospheric plasma density variations in the upper ionosphere with scales ~ 500 km, which are typical of traveling ionospheric disturbances. Thus, both in the lower and upper ionosphere during the active phase of cyclones there are ionospheric plasma variations characteristic of propagating IGWs.

Cyclone-generated IGWs under favorable conditions (more precisely, with a wind structure suitable for propagation into the ionosphere [Medvedev et al., 2017]), reach the lower part of the ionospheric F layer, where they can cause variations in both VLF-signal phase, amplitude and plasma density at Swarm orbital heights. Indeed (see [Shalimov and Solovieva, 2022]), the polarization electric fields arising from wave motion of plasma in the lower part of the F layer (when the wave propagates across the geomagnetic field), projected along geomagnetic field lines to the lower ionosphere, cause the upper wall of the Earth—ionosphere waveguide to rise or fall, i.e. are responsible for VLF-signal phase variations.

The same polarization electric fields perpendicular to the geomagnetic field will lead to plasma drift in the F-region of the ionosphere, i.e. to rise or fall of the plasma column, which, with sufficiently slow motions characteristic of IGWs (with a period of the order of recombination time), will be accompanied by an increase or decrease in electron density on scales of the order of IGW wavelength. These plasma density variations can be detected by a Swarm satellite.

We can assess consistency of satellite measurements with measurements by the VLF radio sounding method. The spatial scales L of density variations observed by the satellite are estimated using the formula $L = v_s/f$, where v_s is the satellite velocity; f is the frequency of variations. Using Figures 6, 7, and 10 to determine scales of plasma density variations, we get $L = 400$ – 600 km. The observed frequencies of wave variations in the lower ionosphere are assumed to correspond to IGWs propagating through the ionosphere; therefore, the estimate $T = T_B \lambda_y / \lambda_z$ is valid for them, where T_B is the Brunt-Väisälä period; λ_z , λ_x are the vertical and horizontal wavelengths. According to model calculations [Vadas and Fritts, 2006], in the thermosphere IGWs generated by convective motions in the atmosphere have vertical wavelengths $\lambda_z \approx 45$ – 55 km. Thus, periods of these waves should occupy the range 30–50 min, which agrees with the VLF radio sounding data (see Figures 4, 5, 9).

The short-period wave variations discussed above are attributed to IGW propagation, so we can assume that long-period variations are also somehow caused by the presence of IGWs, or rather by dissipation of internal waves [Shalimov et al., 2023a].

Indeed, if a cyclone is a source of IGWs propagating to the ionosphere, dissipation of these waves in the lower ionosphere leads to an increase in the coefficient of turbulent diffusion and hence to a faster height redistribution of neutral atmospheric components. A possible response of the ionosphere may be a several-fold decrease in the electron density in the altitude range 60–80 km due to an increase in ozone concentration [Vanina-Dart et al., 2008]. In VLF phase variations, this effect would have corresponded to a negative half-wave lasting several hours and to a rise of the D layer [Shalimov et al., 2023a].

Another process, also driven by IGW dissipation, can be associated with the vertical transfer of NO molecules from the region of their active formation (100–150 km), which causes the electron density in the lower ionosphere to increase [Danilov et al., 1987]. This effect with a characteristic time of several hours may be peculiar to a positive half-wave in VLF phase variations [Shalimov et al., 2023a].

Moreover, IGWs can directly affect the lower ionosphere, thereby, due to the specificity of plasma at these altitudes (electrons are magnetized, but ions are not), resulting in a vertical redistribution of plasma by wind shear (formation of sporadic layers in the E-region [Kelley, 1989]). It can, however, be shown that when IGWs affect the D-region the vertical plasma redistribution (which is necessary to explain VLF-signal phase and amplitude variations) is virtually absent (see, e.g., [Haldoupis, Shalimov, 2021]).

Thus, studies of the ionospheric response to the passage of extratropical cyclones, using a regional network of VLF radio sounding stations and low-orbit satellites (Swarm), allow us to establish that IGWs generated by a cyclone and reaching the ionosphere under favorable conditions can cause variations in both the VLF-signal phase and amplitude and the plasma density in the upper ionosphere, with the structure of responses demonstrating that internal waves from different sources can interact.

The research was carried out under the Government assignment of IPE RAS and MSU. Swarm data was analyzed using software developed under the Government assignment of MSU, theme 01200408544. The work used data from the Unique Research Facility “Seismic and Ultrasonic Monitoring Complex of the Arctic Cryolithozone and Continuous Seismic Monitoring Complex of the Russian Federation, Neighboring Territories, and the World” [<https://ckp-rf.ru/usu/507436/>, <http://www.gsras.ru/unu>]. Characteristics of extratropical cyclones were calculated under RSF project No. 24-17-00138.

REFERENCES

- Akperov M.G., Bardin M.Yu., Volodin E.M., Golitsyn G.S., Mokhov I.I. Probability distributions for cyclones and anticyclones from the NCEP/NCAR reanalysis data and the INM RAS climate model. *Izvestiya, Atmospheric and Oceanic Physics*. 2007, vol. 43, no. 6, pp. 705–712. DOI: [10.1134/S0001433807060047](https://doi.org/10.1134/S0001433807060047).

- Bardin M.Yu., Polonsky A.B. North Atlantic Oscillation and synoptic variability in the European-Atlantic region in winter. *Izvestiya, Atmospheric and Oceanic Physics*. 2005, vol. 41, no. 2, pp. 127–136.
- Bertin F., Testud J., Kersley L. Medium-scale gravity waves in the ionospheric F-region and their possible origin in weather disturbances. *Planet. Space Sci.* 1975, vol. 23, pp. 493–507.
- Chernigovskaya M.A., Kurkin V.I., Orlov I.I., Sharkov E.A., Pokrovskaya I.V. Study of coupling of the ionospheric parameter short period variations in the North Eastern region of Russia with manifestation of tropical cyclones. *Issledovanie Zemli iz kosmosa* [Izvestiya. Atmospheric and Oceanic Physics]. 2010, no. 5, pp. 32–41. (In Russian).
- Chernogor L.F. A tropical cyclone or typhoon as an element of the Earth–atmosphere–ionosphere–magnetosphere system: Theory, simulations, and observations. *Remote Sens.* 2023, vol. 15, iss. 20, 4919. DOI: [10.3390/rs15204919](https://doi.org/10.3390/rs15204919).
- Chou M.Y., Lin C.H., Yue Jia, Tsai H.F., Sun Y.Y., Liu J.Y., Chen C.H. Concentric traveling ionosphere disturbances triggered by Super Typhoon Meranti (2016). *Geophys. Res. Lett.* 2017a, vol. 44, pp. 1219–1226. DOI: [10.1002/2016GL072205](https://doi.org/10.1002/2016GL072205).
- Chou M.Y., Lin C.H., Jia Yue, Chang L.C., Tsai H.F., Chen C.H. Medium-scale traveling ionospheric disturbances triggered by Super Typhoon Nepartak (2016). *Geophys. Res. Lett.* 2017b, vol. 44, pp. 7569–7577. DOI: [10.1002/2017GL073961](https://doi.org/10.1002/2017GL073961).
- Danilov A.D., Kazimirovskii E.S., Vergasova, G.V., Khachikyan G.Ya. Meteorologicheskie efekty v ionosphere [Meteorological Effects in the Ionosphere]. Leningrad, Gidrometeoizdat Publ., 1987, 267 p. (In Russian).
- Das B., Sen A., Pal S., Haldar P.K. Response of the sub-ionospheric VLF signals to the super cyclonic storm Amphan: First observation from Indian subcontinent. *J. Atmos. Solar-Terr. Phys.* 2021, vol. 220, 105668. DOI: [10.1016/j.jastp.2021.105668](https://doi.org/10.1016/j.jastp.2021.105668).
- Dyagilev R.A., Sdelnikova I.A. Unique large-scale research facilities “Seismic infrasound array for monitoring arctic cryolithozone and continuous seismic monitoring of the Russian Federation, neighbouring territories and the world”. *Geodynamics and Tectonophysics*. 2022, vol. 13, no. 2, 0591. DOI: [10.5800/GT-2022-13-2-0591](https://doi.org/10.5800/GT-2022-13-2-0591). (In Russian).
- Forbes J.M., Palo S.E., Zhang X. Variability of the ionosphere. *J. Atmos. Solar-Terr. Phys.* 2000, vol. 62, pp. 685–693. DOI: [10.1016/S1364-6826\(00\)00029-8](https://doi.org/10.1016/S1364-6826(00)00029-8).
- Golitsyn G.S., Mokhov I.I., Akperov M.G., Bardin M.Yu. Distribution functions of probabilities of cyclones and anticyclones from 1952 to 2000: An instrument for the determination of global climate variations. *Doklady Earth Sciences*. 2007, vol. 413, no. 2, pp. 324–326. DOI: [10.1134/S1028334X07020432](https://doi.org/10.1134/S1028334X07020432).
- Haldoupis C., Shalimov S. On the altitude dependence and role of zonal and meridional wind shears in the generation of E region metal ion layers. *J. Atmos. Solar-Terr. Phys.* 2021, vol. 214, 105537. DOI: [10.1016/j.jastp.2021.105537](https://doi.org/10.1016/j.jastp.2021.105537).
- Kelley M.C. *The Earth’s Ionosphere: Plasma Physics and Electrodynamics*. Academic Press, 1989, 500 p.
- Khromov S.P., Petrosyants M.A. *Meteorologia i klimatologia* [Meteorology and Climatology]. Moscow, Nauka Publ., 2006, 582 p. (In Russian).
- Kleimenova N.G., Kozyreva O.V., Rozhnoy A.A., Solov’eva M.S. Variations in the VLF signal parameters on the Australia–Kamchatka radio path during magnetic storms. *Geomagnetism and Aeronomy*. 2004, vol. 44, no. 3, pp. 354–361.
- Lutgens F.K., Tarbuck E.J., Herman R.L. *The Atmosphere. An Introduction to Meteorology*. 14 Edition. New York, Pearson, 2018, 1912 p.
- Medvedev A.V., Ratovsky K.G., Tolstikov M.V., Oinats A.V., Alsatkin S.S., Zhrebtsov G.A. Relation of internal gravity wave anisotropy with neutral wind characteristics in the upper atmosphere. *J. Geophys. Res.: Space Phys.* 2017, vol. 122, pp. 7567–7580. DOI: [10.1002/2017JA024103](https://doi.org/10.1002/2017JA024103).
- Neu U., Akperov M.G., Bellenbaum N., Benestad R., Blender R., Caballero R., Cocozza A., Dacre H.F., et al. IMLAST: a community effort to intercompare extratropical cyclone detection and tracking algorithms. *Bull. American Meteorological Soc.* 2013, vol. 94, no. 4, pp. 529–547. DOI: [10.1175/BAMS-D-11-00154.1](https://doi.org/10.1175/BAMS-D-11-00154.1).
- Olsen N., Friis-Christensen E., Floberghagen R., Alken P., Beggan C.D., Chulliat A., Doornbos E., et al. The Swarm Satellite Constellation Application and Research Facility (SCARF) and Swarm data products. *Earth, Planets and Space*. 2013, vol. 65, pp. 1189–1200.
- Pal S., Sarkar Sh., Midya S.K., Mondal S.K., Hobara Y. Low-latitude VLF radio signal disturbances due to the extremely severe cyclone Fani of May 2019 and associated mesospheric response. *J. Geophys. Res.: Space Phys.* 2020. Vol. 125, iss. 5, e2019JA027288, 11 p. DOI: [10.1029/2019JA027288](https://doi.org/10.1029/2019JA027288).
- Polyakova A.S., Perevalova N.P. Investigation into impact of tropical cyclones on the ionosphere using GPS sounding and NCEP/NCAR reanalysis data. *Adv. Space Res.* 2011, vol. 48, iss. 7, pp. 1196–1210. DOI: [10.1016/j.asr.2011.06.014](https://doi.org/10.1016/j.asr.2011.06.014).
- Rozhnoi A., Solovieva M., Levin B., Hayakawa M., Fedun V. Meteorological effects in the lower ionosphere as based on VLF/LF signal observations. *Natural Hazards and Earth System Sciences*. 2014, vol. 14, iss. 10, pp. 2671–2679. DOI: [10.5194/nhess-14-2671-2014](https://doi.org/10.5194/nhess-14-2671-2014).
- Shalimov S.L., Solovieva M.S. Ionospheric response to the passage of typhoons observed by subionospheric VLF radio signals. *Solar-Terr. Phys.* 2022, vol. 8, iss. 3, pp. 51–57. DOI: [10.12737/stp-83202208](https://doi.org/10.12737/stp-83202208).
- Shalimov S.L., Zakharov V.I., Solov’eva M.S., Bulatova N.R., Korkina G.M., Sigachev P.K. Response of the ionosphere to strong tropospheric disturbances. *Izvestiya. Atmospheric and Oceanic Physics*. 2023a, vol. 59, pp. 1326–1336. DOI: [10.1134/S0001433823120216](https://doi.org/10.1134/S0001433823120216).
- Shalimov S.L., Zakharov V.I., Solov’eva M.S., Sigachev P.K. Wave perturbations of the lower and upper ionosphere during the 2019 Faxai tropical typhoon. *Geomagnetism and Aeronomy*. 2023b, vol. 63, no. 2, pp. 186–196. DOI: [10.1134/S0016793222600576](https://doi.org/10.1134/S0016793222600576).
- Shved G.M. *Vvedenie v dinamiku i energetiku atmosfery* [Introduction to the Dynamics and Energetics of the Atmosphere]. SPbU Publ., 2020, 396 p. (In Russian).
- Simmonds I., Keay K. Extraordinary September Arctic sea ice reductions and their relationships with storm behavior over 1979–2008. *Geophys. Res. Lett.* 2009, vol. 36, no. 19, L19715, pp. 1–5. DOI: [10.1029/2009GL039810](https://doi.org/10.1029/2009GL039810).
- Ulbrich U., Leckebusch G.C., Grieger J., Schuster M., Akperov M., Bardin M.Yu., Feng Ya., Gulev S., et al. Are greenhouse gas signals of Northern Hemisphere winter extra-tropical cyclone activity dependent on the identification and tracking methodology? *Meteorologische Zeitschrift*. 2013, vol. 22, pp. 61–68. DOI: [10.1127/0941-2948/2013/0420](https://doi.org/10.1127/0941-2948/2013/0420).
- Vadas S.L., Fritts D.C. Influence of solar variability on gravity wave structure and dissipation in the thermosphere from tropospheric convection. *J. Geophys. Res.* 2006, vol. 111, A10S12. DOI: [10.1029/2005JA011510](https://doi.org/10.1029/2005JA011510).
- Vanina-Dart L.B., Sharkov E.A. Main results of recent investigations into the physical mechanisms of the interaction

- of tropical cyclones and the ionosphere. *Izvestiya, Atmospheric and Oceanic Physics*. 2016, vol. 52, no. 9, pp. 1120–1157. DOI: [10.1134/S0001433816090279](https://doi.org/10.1134/S0001433816090279).
- Vanina-Dart L.B., Pokrovskaya I.V., Sharkov E.A. Response of the lower equatorial ionosphere to string tropospheric disturbances. *Geomagnetism and Aeronomy*. 2008, vol. 48, no. 2, pp. 245–250. DOI: [10.1134/s001679320802014x](https://doi.org/10.1134/s001679320802014x).
- Yasyukevich Yu.V., Edemskii I.K., Perevalova N.P., Polyakova A.S. *Otklik ionosfery na gelio- i geofizicheskie vozmushchayushchie faktory po dannym GPS* [Ionospheric Response to Helio- and Geophysical Disturbing Factors According to GPS Data]. Irkutsk, Irkutsk State University Publ., 2013, 160 p. (In Russian).
- Zakharov V.I., Kunitsyn V.E. Regional features of atmospheric manifestations of tropical cyclones according to ground-based GPS network data. *Geomagnetism and Aeronomy*. 2012, vol. 52, no. 4, pp. 533–545. DOI: [10.1134/S001679321204016](https://doi.org/10.1134/S001679321204016).
- Zakharov V.I., Pilipenko V.A., Grushin V.A., Khamidullin A.F. Impact of typhoon Vongfong 2014 on the ionosphere and geomagnetic field according to SWARM satellite data: 1. Wave disturbances of ionospheric plasma. *Solar-Terr. Phys.* 2019, vol. 5, iss. 2, pp. 101–110. DOI: [10.12737/stp-52201914](https://doi.org/10.12737/stp-52201914).
- URL: <https://ckp-rf.ru/usu/507436/> (accessed October 22, 2024).
- URL: <http://www.gsras.ru/unu> (accessed October 22, 2024).
- URL: <http://ultramsk.com> (accessed October 22, 2024).
- URL: <http://directory.eoportal.org/web/eoportal/satellite-missions/s/Swarm> (accessed April 22, 2024).
- Original Russian version: Zakharov V.I., Solovieva M.S., Shalimov S.L., Akperov M.G., Korkina G.M., Bulatova N.R., published in *Solnechno-zemnaya fizika*. 2025, vol. 11, no. 1, pp. 77–87. DOI: [10.12737/szf-111202509](https://doi.org/10.12737/szf-111202509). © 2025 INFRA-M Academic Publishing House (Nauchno-Izdatelskii Tsentr INFRA-M)
- How to cite this article*
Zakharov V.I., Solovieva M.S., Shalimov S.L., Akperov M.G., Korkina G.M., Bulatova N.R. Upper atmosphere response to extratropical cyclones. *Solar-Terrestrial Physics*. 2025, vol. 11, iss. 1, pp. 70–80. DOI: [10.12737/stp-111202509](https://doi.org/10.12737/stp-111202509).